Journal of Catalysis 279 (2011) 241–245

Contents lists available at ScienceDirect

Journal of Catalysis

journal homepage: www.elsevier.com/locate/jcat

Promotion of a copper–zinc catalyst with rare earth for the steam reforming of methanol at low temperatures

Ming-Chung Tsai [a], Jung-Hui Wang [b], Chia-Chieh Shen [b,c,d], Chuin-Tih Yeh [a,b,*]

[a] Department of Chemical Engineering and Material Science, Yuan Ze University, Taoyuan 32003, Taiwan, ROC
[b] Fuel Cell Center, Yuan Ze University, Taoyuan 32003, Taiwan, ROC
[c] Department of Mechanical Engineering, Yuan Ze University, Taoyuan 32003, Taiwan, ROC
[d] Graduate School of Renewable Energy and Engineering, Yuan Ze University, Taoyuan 32003, Taiwan, ROC

ARTICLE INFO

Article history:
Received 4 November 2010
Revised 24 December 2010
Accepted 27 December 2010
Available online 2 March 2011

Keywords:
Hydrogen production
Steam reforming of methanol
Copper–zinc-based catalysts
Rare earths

ABSTRACT

The co-precipitation method was used to prepare a reference catalyst composed of copper/zinc oxide (Cu/Zn), as well as a series of Cu/Zn catalysts promoted by monocomponent rare earth (Cu/mRE–Zn) and bicomponent rare earth (Cu/bRE–Zn). The prepared catalysts were tested in a packed-bed reactor in the production of hydrogen via the steam reforming of methanol (SRM). The experimental SRM performance of the prepared catalysts was compared according to three fundamental criteria: the minimum temperature required for 95% conversion of methanol (T_{95}), the selectivity of CO in the hydrogen-rich gas produced (S_{CO}), and the decay rate (k) at T_{95}. The catalysts followed the performance trend Cu/bRE–Zn > Cu/mRE–Zn > Cu/Zn in the SRM tests. Distinctly high SRM performance, i.e., low values for T_{95} (210 °C), S_{CO} (0.04%), and k (negligible in 16 h), was observed using the Cu/bRE–Zn catalyst. The high performance of Cu/bRE–Zn catalysts was attributed to good adhesion of RE oxides to both CuO and ZnO.

1. Introduction

In the chemical industry, a large feedstock of hydrogen is currently produced from the steam reforming of fossil fuels (such as natural gas and petroleum). However, the delivery (including storage and distribution) of hydrogen fuel is a major barrier to promoting the technology of hydrogen fuel cells [1]. One way to eliminate the delivery barrier is to produce hydrogen by on-site reforming. There are many fuel choices for reforming. Methanol is a primary candidate because of its availability, low cost, high energy density, and high chemical activity [2,3].

The steam reforming of methanol (SRM) is a mildly endothermic reaction for the on-site production of hydrogen:

$$CH_3OH + H_2O \leftrightarrow 3H_2 + CO_2 \Delta H = 49.4\ \text{kJ/mol}. \quad (1)$$

Under equilibrium conditions, the extent of methanol conversion (C_{MeOH}) during SRM increases with increasing reaction temperature (T_R) and ratio of steam to methanol (S/C) in the reaction feed. According to the thermodynamic calculation of SRM equilibrium, the temperature required for $C_{MeOH} = 95\%$ (T_{95}) decreased with increasing S/C ratio in the reaction feed. At S/C = 1.3, a low T_{95} of 120 °C was expected from the equilibrium calculation under a constant pressure of 1 atm.

In practice, kinetic control usually inhibits the conversion of reactants, so that 95% conversion is not achieved at the thermodynamically expected T_{95} within a reasonable reaction time. Development of active catalysts is urgently needed to augment the reaction rate. The literature describes a variety of Cu/Zn-based catalysts developed for the SRM reaction. Copper is the active center in the catalysts for methanol decomposition [4], and zinc oxide plays the role of hydrogen sink [5]. Table 1 introduces some recent SRM studies of different modified Cu/Zn catalysts [6–13]. Column 4 of Table 1 indicates that hydrogen was generally produced from methanol at SRM temperatures of $T_R < 300$ °C. However, $T_{95} > 250$ °C is required for all catalysts used.

In a previous report, we found that Ce is a good promoter for Cu/Zn catalysts [14]. In the literature, Cu/CeO_2 catalyst has also been shown to exhibit good SRM activities [12]. Recently, Umegaki et al. used an Artificial Neural Network method to optimize the Cu-based catalysts for oxidative steam reforming of methanol (OSRM) [4]. They found that Cu catalysts promoted by Pr and Ti displayed a low T_{95} (200 °C) and concentration of CO (510 ppm). In this report, our progress in the promotion of Cu/Zn catalysts by various rare earth (RE) elements is introduced. The T_{95} for the SRM can be decreased tremendously to 210 °C, and the selectivity for CO (S_{CO}) and decay rate of the RE-promoted catalysts (Cu/RE–Zn) were also found to decrease with appropriate RE promotion. Also, promotion of Cu/Zn catalysts with bicomponent RE showed better SRM performance than that with monocomponent RE.

* Corresponding author. Fax: +886 4559373.
E-mail address: ctyeh@saturn.yzu.edu.tw (C.-T. Yeh).

0021-9517/$ - see front matter © 2011 Elsevier Inc. All rights reserved.
doi:10.1016/j.jcat.2010.12.018

Table 1
A summary on recent reports on the SRM reaction.

Catalyst	S/C ratio	WHSV (h^{-1})	T_{95} (°C)	S_{CO} (%)	Reference
Cu/ZnZrAl	1.1	7.6	270	0.3	Huang et al. [5]
Cu/ZnAl	1.0–1.5	0.5	260–280	3.4–6.0	Takeda et al. [6]
Cu based	1.5	~0.1	280	>1.2	de Wild et al. [7]
Cu/ZnAl	1.3	26.0	310	None	Agrell et al. [8]
Cu/ZrZnAl	1.3	2.8	350	2.0	Breen et al. [9]
Cu/Al	1.0	50.0	400	0.8	Segal et al. [10]
Cu/CeZnAl	1.4	11.0	280	0.6	Patel et al. [11]
Cu/Ce	1.5	0.3	280	>6.0	Udani et al. [12]
Cu/CeZn	1.3	4.0	300	6.3	Hong et al. [13]

2. Materials and methods

2.1. Sample preparation

The conventional co-precipitation method was employed to prepare a reference copper–zinc (Cu/Zn) catalyst as well as a series of RE-promoted Cu/Zn (Cu/RE–Zn) catalysts. The prepared Cu/RE–Zn catalysts were classified into two categories: promotion using monocomponent or bicomponent RE (Cu/mRE–Zn and Cu/bRE–Zn). Column 1 of Table 2 lists the chemical compositions of the catalysts prepared. The subscript of each metal in the composition indicates the oxide weight ratio in the catalysts. For example, Cu_3/Ce_4–Zn_3 represents a Cu/mRE-Zn catalyst with 30 wt.% CuO, 40 wt.% CeO_2, and 30 wt.% ZnO. The loading of copper oxide in all catalysts prepared was held at 30 wt.%. In Cu/RE–Zn catalysts, including Cu/mRE–Zn and Cu/bRE–Zn, the total loading of RE was fixed at 40 wt.%.

The catalysts were prepared by precipitating a nitrate of each metal with Na_2CO_3 at a pH of 7.5 for 2 h. The resulting precipitates were subsequently filtered, washed with deionized water, and calcined at 400 °C. The calcined catalysts were further crushed and sieved between 45 and 60 meshes and stored for use as fresh catalysts in subsequent studies. Nitrates of three RE elements, Ce, Pr, and Tb, were purchased from Aldrich and used to modify the Cu/Zn catalyst. Aside from the freshly prepared catalysts, the SRM performance of two commercially available catalysts (Comm-G and Comm-M) was tested for comparison.

2.2. Physical characterization of the fresh catalysts

The specific surface areas of the fresh catalysts were estimated (column 2 of Table 2) using nitrogen physisorption measurements (Micromeritics ASAS-2020). A temperature-programmed reduction system (TPR, with a 30 ml/min reductive stream of 10% H_2 in N_2 and a rate of temperature increase of 7 °C/min) was used to examine the reduction behavior of the studied catalysts. A Shimadzu LabX XRD-6000, equipped with a sample stage that could be heated to 300 °C, was used to examine the effects of the reduction temperature on the average diameter of Cu (d_{Cu}) in the fresh catalysts.

2.3. Activity test

The SRM performance was tested in a packed-bed reactor made of a quartz tube with inner diameter 4 mm. A 100-mg catalyst sample was inserted into the reactor and pre-reduced by a stream of H_2 at 250 °C. A reactant mixture of S/C = 1.3 was then supplied by a syringe pump and carried through a 120 °C vaporizer to the catalyst bed by a flow of He (73% in partial molal composition). A contact time of WHSV (methanol) = 10 h^{-1} was maintained for the SRM studies. An input rate of 0.031 mol methanol h^{-1} was then supplied to the reactor. The reactor temperature (T_R) was increased stepwise (at 30 °C/step) from 120 to 270 °C by heating in an oven. The products of the SRM reaction were collected using a loop after 30 min reaction at each T_R and analyzed by thermal conductivity detector-gas chromatography (for the methanol conversion measurements) and by ion-trap mass spectrometry (MS, Thermal Scientific TTQ 700, for CO measurement). The ion-trap MS can sensitively and linearly detect CO concentrations between 5 and 1000 ppm. The C_{MeOH} and S_{CO} of the SRM were calculated from the product distribution according to

$$C_{MeOH} = ([MeOH]_{in} - [MeOH]_{out})/[MeOH]_{in},$$
$$S_{CO} = [CO]_{out}/([CO]_{out} + [CO_2]_{out}).$$

3. Results

3.1. Temperature-programmed reduction characterization

Fig. 1 displays the TPR profiles from the freshly prepared catalysts. The Cu/Zn catalyst displayed a reduction peak of dispersed CuO at T_r = 240 °C. The peak may be assigned to a reduction of support CuO:

$$H_2 + CuO \rightarrow Cu + H_2O. \quad (2)$$

A similar T_r was found from TPR (not shown in Fig. 1) for fine CuO powders ($d \sim 1$ μm) prepared by the precipitation of $CuNO_3$. However, the RE-modified Cu/RE–Zn catalysts were always reduced at low temperatures (T_r < 220 °C). The shift T_r implied an intimate interaction between the RE oxides and the CuO on Cu/RE–Zn catalysts. Temperatures T_r found in Fig. 1 are listed in the fifth column in Table 2 for different catalysts. Notably, a reduction peak at T_r = 190 °C was always found for catalysts promoted with Ce (Cu/CeZn, Cu/CePr–Zn, and Cu/CeTb–Zn), whereas a peak at T_r = 220 °C was found for catalysts promoted with Tb.

Table 2
Results on physical characterization of fresh catalysts and their SRM performance.

Catalyst	S.A. (m^2/g)	Cu (1 1 1) peak		T_r (°C)	SRM performance			
		d (nm)	intensity		T_{95} (°C)	S_{CO} (%)	k (min^{-1})	TOF[a] (s^{-1})
Cu3/Zn7	30	14	100	240	300	0.75	27.5	0.32
Cu3/Ce4–Zn3	93	7.1	6	190	240	0.20	7.6	0.16
Cu3/Tb4–Zn3	55	5.2	15	220	240	0.19	2.8	0.12
Cu3/Pr4–Zn3	72	4.5	5	200	240	0.14	2.5	0.10
Cu3/Ce1Tb3–Zn3	65	3.0	4	190, 220	210	0.05	0.3	0.07
Cu3/Ce1Pr3–Zn3	103	2.5	3	180–190	210	0.04	0.0	0.06
Comm-G	27	15	47	210	300	4.0	0.0	0.34
Comm-M	76	13	77	230	270	2.5	0.0	0.30

[a] TOF at T_{95} based on d_{Cu} from XRD examination.

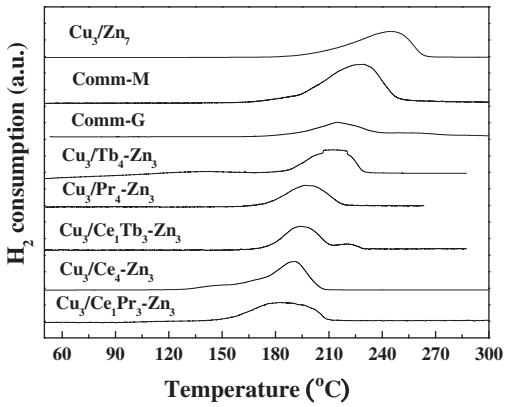

Fig. 1. TPR characterization of Cu catalysts prepared in this study and obtained from the commercial market.

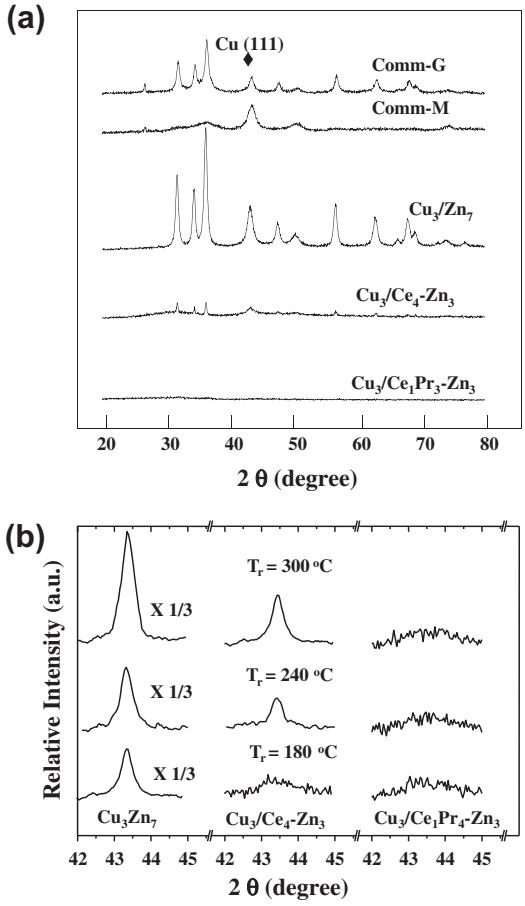

Fig. 2. (a) Comparison of XRD traces of catalysts prepared in this study with those of two commercial catalysts. The catalysts have been pre-reduced by hydrogen at 200°C. (b) Variation of Cu (1 1 1) peak from different fresh sample after 1 h reduction by H_2 at temperatures of 180 (bottom), 240 (middle), and 300 °C (top). Profiles Cu/mRE–Zn and Cu/bRE–Zn represents data from samples of Cu_3/Ce_4–Zn_3 and $Cu/Ce_{10}Pr_3$–Zn_3, respectively.

3.2. XRD characterization

Fig. 2a compares the XRD traces for two commercial catalysts (Comm-G and Comm-M) with those for three representative catalysts (Cu_3/Zn_7, Cu_3/Ce_4–Zn_3, and Cu_3/Ce_1Pr_3–Zn_3). The latter three catalysts were used in this work to represent the reference Cu/Zn, RE-modified Cu/mRE–Zn, and Cu/bRE–Zn. A stream of hydrogen was used to reduce the catalysts in situ in the XRD chamber at 200°C, prior to the trace collection. Traces from the representative catalysts arose mainly from the Cu (1 1 1) peak (2 = 43°) and the XRD peaks of ZnO. Negligible diffraction from the RE components was observed for the RE-modified catalysts. However, peaks from the RE oxides and the spinels of CuRE mixed oxides did appear in the XRD traces of the Cu/RE–Zn catalysts (not shown in the figure) after calcination at elevated temperatures (600 °C and higher). Apparently, the RE oxides were finely dispersed in an XRD amorphous state on the fresh Cu/RE–Zn but sintered into crystallites upon calcination at high temperatures.

Fig. 2b compares the Cu (1 1 1) peaks for the three representative catalysts. They had been pretreated in situ in the XRD compartment by a hydrogen stream for 1 h at 180, 240, and 300 °C prior to XRD characterization. Upon the initial treatment at 180 °C (bottom of Fig. 2b), the reference Cu/Zn catalyst (shown at the left in Fig. 2b) displayed a strong peak, whereas the peaks of Cu/Ce–Zn and Cu/CePr–Zn were relatively weak and broad. Column 3 of Table 2 lists the diameter of Cu particles (d_{Cu}) estimated from the Scherrer equation for fresh catalysts reduced at 180 °C. The reference Cu/Zn had a large d_{Cu} of 14 nm. The d_{Cu} of the RE-modified catalysts was quite small, 5.6 1.0 nm for Cu/mRE–Zn (Cu/Ce–Zn, Cu/Tb–Zn, and Cu/Pr–Zn) and 2.8 0.3 nm for Cu/bRE–Zn (Cu/CePr–Zn and Cu/CeTb–Zn). Although the loading of Cu on the fresh catalysts was similar (30 wt.%), the intensity of the Cu (1 1 1) peak in the XRD traces varied with the sample composition. The area of the Cu (1 1 1) peak from the Cu/Zn was substantially larger (by a factor of 3 or more) than that of those from the RE-modified catalysts. Conceivably, a major fraction of copper on the modified catalysts existed in an amorphous form ($d_{Cu} < 2$ nm) after reduction at 180 °C.

Metal particles dispersed on the metallic catalysts tended to sinter at high temperatures under hydrogen. Fig. 2b displays the influence of the hydrogen treatment temperature on the Cu (1 1 1) peaks of three representative catalysts. The three peaks (bottom, middle, and top) on the left-hand side of the figure indicate that the peak intensity of the reference Cu/Zn increased with increasing temperature of treatment. Conceivably, a substantial fraction of the reduced Cu on the fresh Cu/Zn was dispersed in an amorphous state (with $d_{Cu} < 2$ nm) upon reduction at 180 °C. The amorphous Cu on the catalysts tended to sinter (to $d_{Cu} \sim 14$ nm) during high-temperature reduction:

$$\text{Amorphous Cu} \rightarrow \text{Crystalline Cu}(d \sim 14\ \text{nm}). \quad (3)$$

The sintering of amorphous Cu (process 3) during hydrogen treatment was also observed in Fig. 2b for the RE-promoted (Cu/RE–Zn) catalysts. However, the extent of Cu sintering was significantly diminished in Cu/mRE–Zn and became negligible for Cu/bRE–Zn.

3.3. SRM performance

Fig. 3 compares the temperature profiles of C_{MeOH} over three representative catalysts and two commercial catalysts (Comm-G and Comm-M) available. The observed C_{MeOH} from these catalysts generally increased with increasing reaction temperature. The comparison showed that the SRM activity of Cu/Zn catalysts prepared in this study was inferior to that of commercial catalysts. However, activities of the fresh catalysts promoted by RE, Cu/mRE–Zn (data from Cu_3/Ce_4–Zn_3) and Cu/bRE–Zn (data from Cu_3/Tb_3Ce_1–Zn_3), were always superior to those of commercial catalysts. Column 6 of Table 2 compares the experimentally observed T_{95} temperatures for all freshly prepared catalysts. The T_{95} of the Cu/Zn catalyst was substantially decreased by promotion with RE.

A low T_{95} not only conserves energy during operation of the reformer, but also is beneficial to its integration with a hydrogen fuel

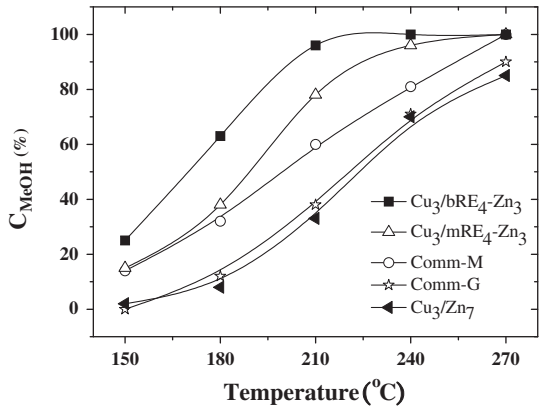

Fig. 3. Temperature profiles of C_{MeOH} of SRM over the representative prepared catalysts and commercial catalysts GandM.

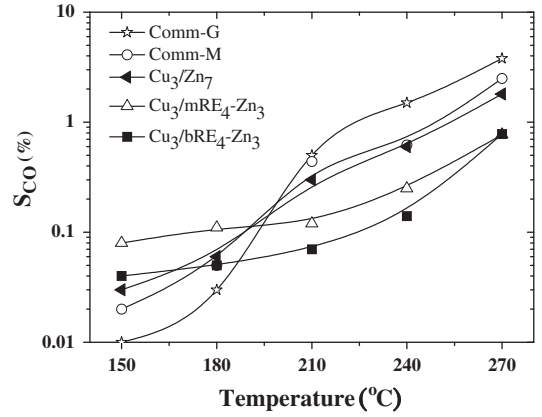

Fig. 4. Temperature profiles of SCO from SRM over the representative catalysts and the commercial catalysts.

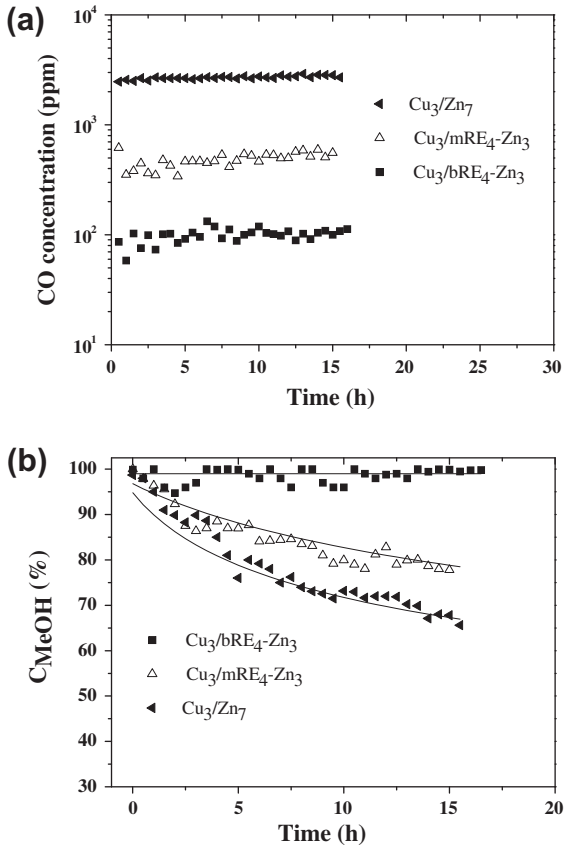

Fig. 5. Temperature profiles of (a) CO concentration and (b) C_{MeOH} in SRM over the representative catalysts at their T95 temperatures. The solid curves in (b) are theoretical simulated profiles using the rate constant k listed in the next to last column of Table 2.

cell for the generation of electric power [15,16]. It should be noted that the Cu/bRE–Zn catalysts (Cu/CePr–Zn and Cu/CeTb–Zn) generally exhibited a low T_{95} of 210 °C. To the best of our knowledge, this T_{95} represents the lowest temperature recorded (on comparison with data in column 4 of Table 1) for 95% methanol conversion during SRM. However, the T_{95} (210 °C) of Cu/bRE–Zn remained higher than the 120 °C, expected from the equilibrium of SRM with S/C = 1.3. Further improvement and development for advanced SRM catalysts are therefore strongly encouraged.

Hydrogen, carbon dioxide, and carbon monoxide were the major products detected from our SRM tests. Minor amounts of methyl formate were also detected by the ion-trap MS as a byproduct at high SRM temperatures (T_R > 270 °C). At T_R < 270 °C, the methyl formate signal became negligible. Fig. 4 plots the temperature dependence of S_{CO}, analyzed by MS. The experimental S_{CO} increased with T_R, but varied according to the catalysts used. In agreement with a literature report [12], the experimental S_{CO} in the SRM is always lower than the theoretical expectation (for example, S_{CO} = 10% at 240 °C and S/C = 1.3) from the equilibrium of the water–gas shift reaction (WGSR). The discrepancy in S_{CO} suggests that CO is a byproduct of SRM, and that the WGSR was far from equilibrium under the SRM conditions of this study.

The seventh column of Table 2 compares the S_{CO} measured for fresh catalysts at their respective T_{95} temperatures. The comparison suggests that promotion of Cu/Zn by RE also decreased S_{CO} in the SRM. A CO selectivity S_{CO} < 0.1% was generally found for Cu/bRE–Zn catalysts. This S_{CO} was significantly lower than those (>2%) found for commercial catalysts (see Table 1). A low S_{CO} in reformed hydrogen is strongly desired to improve the coupling of reformers to hydrogen fuel cells during electricity generation [16].

The SRM performance of fresh catalysts was tested for 16 h to measure their long-term stability during SRM at their respective T_{95}. Fig. 5a shows that S_{CO} increased only slightly during the time range studied. However, a significant decrease in C_{MeOH} was observed from the reference catalyst Cu/Zn at its T_{95} (Fig. 5b). The conversion decrease for catalytic reactions has been suggested by Kung et al. to follow an empirical equation [17],

$$(C_0/C_t)^{1/n} = 1 + kt, \quad (4)$$

where C_0 denotes the initial conversion (at t = 0), C_t denotes the methanol conversion at time t, n is an empirical parameter (~0.2), and k is a constant that describes the decay rate during reaction. The decay constant k was simulated for all C_{MeOH} profiles shown in Fig. 5b using n = 0.2. Fair agreement between the simulated profiles (solid line) and the experimentally determined C_{MeOH} (data points) was found. The decay constants simulated for the prepared catalysts are listed in the eighth column of Table 2. The decay rates for the prepared Cu/Zn catalysts also decreased with the RE promotion. Notably, the conversion C_{MeOH} of Cu/bRE–Zn in the durability test scattered between 94% and 100% at the initial 10 h and remained > 98% after t > 10 h at its low T_{95} temperature 210 °C. A decay constant of k = 0 was therefore assigned for Cu/bRE–Zn at T_{95}.

4. Discussion

Copper metal on Cu/Zn-based catalysts provides the active sites for SRM reactions. Accordingly, the SRM activity over Cu catalysts

generally increases with the number of copper sites [18]. High Cu-loaded (>30 wt.%) catalysts are therefore prepared for good SRM activity. The profiles of C_{MeOH}, shown in Fig. 3, indicate that the T_{95} required for the fresh catalysts with a constant Cu loading of 30 wt.% was reduced by promotion with RE. The good SRM activity of the Cu/RE–Zn catalysts may be attributed to their high Cu dispersion (or small d_{Cu}).

A major portion of copper crystallites on the reference Cu/Zn was quite large (d_{Cu} = 14 nm). Fig. 1 indicates that a reduction peak at T_r = 240°C was found for the reduction of CuO from the fresh Cu/Zn. A similar T_r has been found from bulk CuO. The similarity in T_r temperature suggested that the interaction between CuO and ZnO on the reference catalyst Cu/Zn was weak. The large d_{Cu} should have resulted from the high 30 wt.% Cu loading and weak interactions between the ZnO support and the supported CuO. The oxides tended to precipitate and crystallize separately, due to their relatively strong cohesive forces, into large particles (>10 nm) during preparation. A small surface area (30 m^2/g) was therefore found in column 2 of Table 2 for the fresh Cu/Zn.

The extent of interaction between the dispersed CuO and the support on catalysts may be characterized by T_r, the temperature of reduction of CuO by hydrogen. Fig. 1 indicates that T_r of Cu/RE–Zn catalysts was lower than that (240 °C) of unsupported CuO. A shift of the reduction temperature CuO on CeO_2 promoted copper catalysts to T_r < 200°C has also been reported in TPR studies [5,12]. The shift was attributed to the interaction of CuO with CeO_2. Accordingly, the decrease in T_r on Cu/RE–Zn can be attributed to a strong interaction between CuO and RE. From the T_r variation in the fifth column of Table 2, the interaction between CuO with supports generally increased following a trend of

$$\mathrm{Cu/Zn} < \mathrm{Cu/mRE-Zn} < \mathrm{Cu/bRE-Zn}, \quad \text{(I)}$$

where Cu/mRE–Zn indicates Cu_3/Ce_4–Zn_3, Cu_3/Tb_4–Zn_3, and Cu_3/Pr_4–Zn_3, whereas Cu/bRE–Zn includes Cu_3/Ce_1Pr_3–Zn_3 and Cu_3/Ce_1Tb_3–Zn_3. Interestingly, a similar trend was also observed in the SRM performance including T_{95}, S_{CO}, and the value of k at T_{95} (columns 6, 7, and 8 in Table 2).

The XRD results of Fig. 2 indicate that d_{Cu} decreased with increasing interaction between Cu and RE (trend I). The RE in catalysts Cu/RE–Zn therefore acted as a texture promoter that prevented the formation of large crystallites of ZnO and CuO during preparation. High surface areas (>55 m^2/g) and highly dispersed Cu were therefore observed (columns 2 and 3 of Table 2) for Cu/RE–Zn catalysts. Although the amount of RE oxides on Cu/mRE–Zn and Cu/bRE–Zn catalysts is the same (30 wt.%), the size of RE oxides in Cu/bRE–Zn catalysts became finer because of an increasing heterogeneity in composition. Consequently, Cu/bRE–Zn catalysts had a higher D_{Cu} and exhibited better SRM performance.

The last column of Table 2 lists TOF of methanol over different catalysts (based on d_{Cu} in column 3 of Table 2) at their T_{95} temperatures. The listed TOFs varied with catalysts tested and generally increased with their T_{95}. At a fixed reaction temperature of 210 °C, however, a similar TOF of 0.11 0.06 s^{-1} was obtained from all of the catalysts. The small variation in TOF at constant T_R = 210 °C suggests that the SRM activity of copper sites on Cu/RE–Zn did not change with RE promotion. The RE promotion observed for Cu/RE–Zn catalysts may be attributed mainly to an increase in the number of active sites.

The fresh Cu/bRE–Zn catalysts displayed long-term stability when applied to SRM (Fig. 5b). Sintering of Cu was considered to be the major reason for the decay of Cu/ZnO-based catalysts during SRM [12]. The promoted stability therefore may also be attributed to strong interactions between RE oxides and Cu. XRD results shown in Fig. 2b indeed indicated negligible sintering of Cu particles in Cu/bRE–Zn under H_2 within the temperature range of our SRM study (<300 °C). The stability of the RE-modified catalysts during SRM reactions could, therefore, be attributed to the slow rate of Cu sintering (process 3).

The seventh column of Table 2 indicates that all fresh catalysts prepared showed a significantly lower S_{CO} (<0.75%) than the commercial catalysts (>2%) at T_{95}. The high S_{CO} of the commercial catalysts was partially attributed to the Al_2O_3 component added (for lifetime stability enhancement) [5]. However, S_{CO} was found in Fig. 4 to increase with increasing T_R of SRM. The low S_{CO} (0.1% or less) of the RE-modified catalysts Cu/RE–Zn may be attributed mainly to their low required T_{95}.

5. Conclusion

Several 30 wt.% Cu/RE–Zn catalysts modified with different RE were prepared for the production of hydrogen via the SRM. Their SRM performances were compared according to three fundamental criteria: T_{95}, S_{CO}, and durability. The prepared catalysts showed the following general trends based on the three criteria:

$$\mathrm{Cu/bRE-Zn} > \mathrm{Cu/mRE-Zn} > \mathrm{Cu/Zn}.$$

Evidently, RE is a good promoter of Cu/Zn catalysts for SRM, and bicomponent RE additions generally display better promotion effects than monocomponent RE. The catalyst promotion by RE was attributed to strong interactions between the RE oxide and both ZnO and the supported Cu. In addition, dramatically low T_{95} (210 °C) and S_{CO} (0.1%) were found for the SRM over the Cu/bRE–Zn catalysts (Cu/CePr–Zn and Cu/CeTb–Zn). Employment of the Cu/bRE–Zn catalysts developed in a SRM reformer should be advantageous for coupling to a hydrogen fuel cell to generate electric power.

Acknowledgment

This work was supported by the National Science Council of Taiwan under Contract NSC-98-2627-M-155.

References

[1] C. Song, Catal. Today 77 (2002) 17.
[2] T. Conant, A.M. Karim, V. Lebarbier, Y. Wang, F. Girgsdies, R. Schlogl, A. Datye, J. Catal. 257 (2008) 64.
[3] J. Larminie, A. Dicks, Fuel Cell System Explained, second ed., Wiley, West Sussex, England, 2003.
[4] T. Umegaki, A. Masuda, K. Omata, M. Yamada, Appl. Catal. A: Gen. 351 (2008) 210.
[5] G. Huang, B.J. Liaw, C.J. Jhang, Y.Z. Chen, Appl. Catal. A: Gen. 358 (2009) 7.
[6] K. Takeda, A. Baba, Y. Hishinuma, T. Chikahisa, JSAE Rev. 23 (2002) 183.
[7] P.J. de Wild, M.J.F.M. Verhaak, Catal. Today 60 (2000) 3.
[8] J. Agrell, H. Birgersson, M. Boutonnet, J. Power Sources 106 (2002) 249.
[9] J.P. Breen, J.R.H. Ross, Catal. Today 51 (1999) 521.
[10] S.R. Segal, K.B. Anderson, K.A. Carrado, C.L. Marshall, Appl. Catal. A: Gen. 231 (2002) 215.
[11] S. Patel, K.K. Pant, J. Power Sources 159 (2006) 139.
[12] P.P.C. Udani, P.V.D.S. Gunawardana, H.C. Lee, D.H. Kim, Int. J. Hydrogen Energy 34 (2009) 7648.
[13] Y. Hong, X.Z. Fu, J.D. Lin, H.B. Chen, D.W. Liao, Xiamen Daxue Xuebao 42 (2003) 60 (Language: Chinese, Database: CAPLUS).
[14] L. Mo, A.H. Wan, X. Zheng, C.T. Yeh, Catal. Today 148 (2009) 124.
[15] T. Kim, S. Kwon, Sens. Actuators A – Phys. 154 (2009) 204.
[16] G. Avgouropoulos, J. Papavasiliou, M.K. Daletou, J.K. Kallitsis, T. Ioannides, S. Neophytides, Appl. Catal. B – Environ. 90 (2009) 628.
[17] E.D. Schrum, T.L. Reitz, H.H. Kung, Stud. Surf. Sci. Catal. 139 (2001) 239.
[18] T. Shishido, Y. Yamamoto, H. Morioka, K. Takehira, J. Mol. Catal. A – Chem. 268 (2007) 185.